Model Predictive Control of a Variable-Speed Pitch-Regulated Wind Turbine

Sung-ho Hur and Bill Leithead
Wind Energy & Control, Department of Electronic and Electrical Engineering
University of Strathclyde, Glasgow, G1 1XZ, UK
Email: hur.s.h@ieee.org

***Abstract*—The Model Predictive Controller is designed for a 5MW variable-speed pitch-regulated wind turbine for three operating points – below rated wind speed, just above rated wind speed, and above rated wind speed. At each operating point, the controllers are designed based on two different linear models of the same wind turbine to investigate the impact of using different control design models (i.e. the model used for designing a model-based controller) on the control performance.**

I. Introduction

A wind turbine converts the kinetic energy from the wind into mechanical energy. It is then converted into electricity, which is subsequently transmitted to a power grid [1]. This paper is concerned with a 5MW variable-speed pitch-regulated horizontal-axis wind turbine, having three blades.

The overall control design steps for designing a control system for regulating variable-speed wind turbines, which are often implemented and pursued in this study, can be briefly summarised as follows:

1) Development of linear control design models at 4 operating points or modes (explained in more detail below)
2) Design of control synthesis based on the design models from Step 1 at each mode
3) Design of control strategy (i.e., switching between the controllers from Step 2, incorporation of a drive-train damper, etc.) to obtain a full-envelope controller
4) Application of the full-envelope controller (from Step 3) to the high-fidelity aero-servo-elastic model, developed in DNV-GL Bladed (Bladed), from which the linear models have been derived. This step tests the controller in terms of all significant variables and loads and lifetime equivalent fatigue load estimates.
5) Application of the full-envelope controller (from Step 4) to the real-life turbine that the aero-elastic model represents by refining the controller.

This paper focuses only on Steps 1 and 2, and the following steps are beyond the scope of this paper. The main objective of this study is to investigate the effect of using different linear control design models in Step 1 on the performance of the control synthesis in Step 2.

The synthesis of the controller design in Step 2 is concerned with designing single input single output (SISO) linear controllers at different operating points. More specifically, linear controllers are often designed at 4 operating points, in the lowest wind speeds (mode 1), in intermediate wind speeds (mode 2), in higher, but still below rated, wind speeds (mode 3) and in above rated wind speeds (mode 4). Note that the rated wind speed is a pre-determined wind speed, at which the limit on power output to the wind turbine (5MW in this paper), is reached. When the wind speed exceeds rated, the excess power in the wind is discarded to prevent the turbine from overloading.

Operating in mode 4 and switching between modes 3 and 4 are more challenging, and thus this paper focuses on modes 3 and 4. In mode 3 one linear controller is designed at a mean wind speed of 10 m/s, and in mode 4 two linear controllers are designed at mean wind speeds of 12 and 14 m/s here.

The linear controllers can be designed using various control methods. The most common one stems from PI control [2] (usually with significant modifications to incorporate fatigue reduction, anti-windup, etc.). In this paper, Model Predictive Control (MPC) [3] is tested. Note that other control methods such as Linear Quadratic Gaussian (LQG) control [4] or H_∞ [5] could also be equally appropriate.

To design such model-based linear controllers in each mode, a control design model [6] is required in each mode. To investigate the effect of exploiting different control design models on the control performance in Step 2, two different control design models are developed and tested. Both control design models are linear models of the Supergen Wind Energy Technologies Consortium (Supergen) 5MW exemplar turbine.

The first linear models are obtained from the (nonlinear) Bladed model of the turbine using its built-in linearisation tool. The second models are obtained by linearising the nonlinear model provided in [2], [7], with the parameters of the same turbine, by the use of the standard linearisation technique via symbolic differentiation. Both linearised models are implemented in Matlab/SIMULINK® to allow the controller design to be performed therein. Throughout the paper, the first linear models are referred to as "Models A", and the second linear models as "Models B". *These linearised models could be provided by the authors upon request; please contact the corresponding author.*

When model-based controllers are designed based on a model (from Step 1), the controllers are first tuned by application to the controller design model itself. For the same reason here, when Models A are exploited as the controller design models, the controllers are tuned by application to Models A, and when Models B are exploited as the controller design

models, the controllers are tuned by application to Models B.

Thus the controllers designed based on Models A (i.e. Models A-based controllers) and the controllers designed based on Models B (i.e. Models B-based controllers) are independent, and there is no direct connection between them. However, for the purpose of comparing the performance of these two controllers, Models A-based controllers are applied to Models B in addition to Models A, and Models B-based controllers to Models A in addition to Models B. The differences between these models provide a degree of model-plant mismatch, which would exist in real life, to test the robustness of design. The results in [8] demonstrate that the application of Models A-based controllers to Models A and Models B produce similar results, and the application of Models B-based controllers to Models A and Models B produce similar results. Hence, this paper only presents the application of Models A-based controllers to Models B and the application of Models B-based controllers to Models A.

The strategy of the controller design (Step 3) is responsible for switching between the linear controllers from Step 2 by an appropriate switching method, yielding a global nonlinear controller that covers the full operational envelop [9]. It is related to nonlinear aspects of the plant dynamics, and an investigation of the global behaviour of the system is required. However, as mentioned previously, the work presented here is only concerned with Steps 1 and 2. Therefore, the nonlinear Bladed turbine model cannot be used as Step 3 has not been performed. If it was used, when the nonlinear model requires the linear controller to switch around at 12 m/s (the rated wind speed), the operation would become unstable because when switching, the nonlinear model would require the linear controller to provide negative control action (pitch angle), which is not physically feasible. Moreover, drive-train and tower dampers [2] need to be designed during Step 3, or the operation would again become unstable.

The main contribution of this paper is to investigate the effect of the control design model on the performance of the controllers, i.e. the effect of utilising Models A in comparison to Models B when designing MPC controllers.

The wind speed model, which is required for simulations, Models A, and Models B are reported in Section II. Section III reports on the MPC controllers including some simulation results in Matlab/SIMULINK. Conclusions are drawn in Section IV.

II. Wind Speed and Linear Models

A. Wind Speed Model

The wind is stochastically varying with time and continuously interacting with the rotor. The effective wind speed is wind speed averaged over the rotor area such that the spectrum of aerodynamic torque remains unchanged. It can be obtained by filtering the point wind speed. The power spectrum for the point wind speed is the Von Karman spectrum [10]

$$S_v(\omega) = 0.476\sigma_v^2 \frac{\frac{L_t}{\bar{V}}}{(1+(\frac{\omega L_t}{\bar{V}})^2)^{5/6}} \tag{1}$$

where $L_t = 6.5h$ denotes the turbulence length of the spectrum, h height, and $\bar{V}$ mean wind speed. σ_v represents turbulence intensity and is assumed to be 18.34, 17.03, and 16.10 % for mean wind speeds of 10, 12, and 14 m/s, respectively.

The Von Karman spectrum can be approximated by the following Dryden spectrum:

$$S_D(\omega) = \frac{1}{2\pi}\frac{b_d^2}{\omega^2+\alpha_d^2} \tag{2}$$

The corresponding point wind speed is modelled by coloured noise as follows:

$$v_d = \frac{\bar{V}b_d}{s+a_d}\xi \tag{3}$$

where ξ denotes Gaussian noise.

For (3), the values of a_d and b_d, for which the Dryden spectrum best approximates the Von Karman spectrum, are

$$a_d = 1.14\frac{\bar{V}}{L_t} \tag{4}$$

$$b_d = \sigma_v\sqrt{2a_d} \tag{5}$$

The effective wind speed is the wind speed actually experienced by the wind turbine. It can be modelled by spatially filtering point wind speed using the following filter:

$$S_p(s) = \frac{\sqrt{2}(\sqrt{2}+\sigma(\hat{V})s)}{(\sqrt{2}+\sqrt{\alpha}\sigma(\hat{V})s)(\sqrt{2}+\sigma(\hat{V})s/\sqrt{\alpha})} \tag{6}$$

α is set to 0.55 [11], and $\hat{V}$ denotes the average wind speed over a period of time equivalent to a small number of rotations of the rotor. It can be derived by filtering the point wind speed through the first order filter

$$S_f(s) = \frac{1}{\tau s+1} \tag{7}$$

τ is the period over which the wind speed is averaged, and $\sigma(\hat{V})$ is given as follows:

$$\sigma = \frac{\gamma R}{\hat{V}} \tag{8}$$

where γ denotes the turbulent wind field decay factor and is set to 1.3. The result from filtering the point wind speed through the spatial filter is shown for a mean wind speed of 10 m/s in Fig. 1. The figure depicts the effective wind speed (in blue) together with the point wind speed (in red). Similar results can be obtained for mean wind speeds of 12 and 14 m/s. The rotor radius (R) and the height of the Supergen 5MW turbine are 60 m and 90 m, respectively.

Nonlinear rotational sampling [12] is subsequently added to the effective wind speed. The equations for the rotational sampling ($\Delta\omega$) are summarised as follows:

$$\Delta\omega = \frac{1.25}{s/(3\Omega_o)+1.25}x_r \tag{9}$$

where Ω_o denotes the operating rotor speed (i.e., 1.23 rad/s), x_r is given as

$$x_r = \epsilon_1 cos(3\Omega_o t) + \epsilon_2 cos(3\Omega_o t) \tag{10}$$

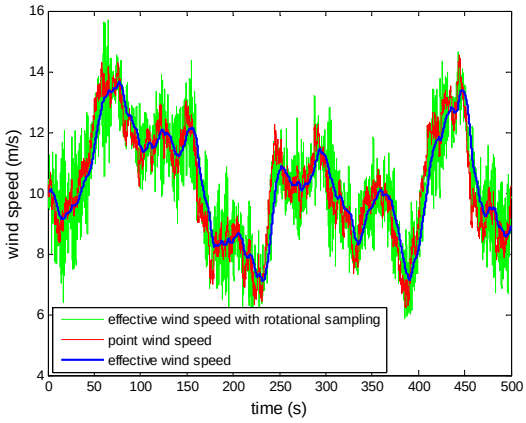

Fig. 1. Point wind speed (red) vs effective wind speed (blue) vs effective wind speed with linear rotational sampling (green) at a mean wind speed of 10 m/s.

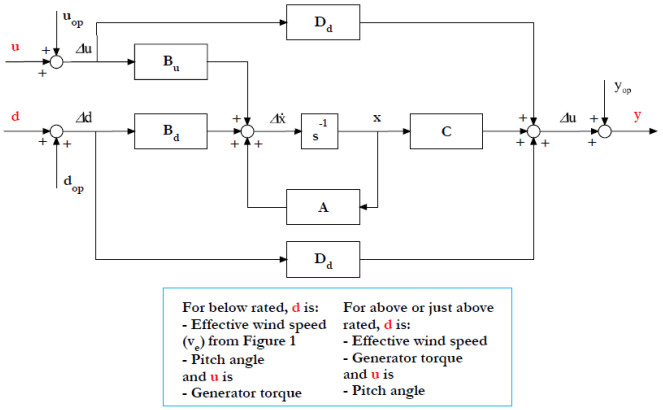

Fig. 2. Linearised wind turbine model.

and

$$\dot{\epsilon}_1 = -a\epsilon_1 + b\xi_1 \tag{11}$$
$$\dot{\epsilon}_2 = -a\epsilon_2 + b\xi_2 \tag{12}$$

ξ_1 and ξ_2 denote Gaussian white noise, and a and b are, respectively, set to 0.4 and 3.

The effective wind speed with and without the effect of rotational sampling are depicted in comparison to the point and effective wind speed for a mean wind speed of 10 m/s in Fig. 1. Similar results are obtained for mean wind speeds of 12 and 14 m/s. The linear wind turbine models exploit the effective wind speed with rotational sampling throughout the paper.

B. Wind Turbine Linear Models A (Bladed Linearisation)

Dynamic models are linearised from the (nonlinear) Bladed model of Supergen 5MW exemplar turbine for three different operating points, below rated wind speed (10 m/s), just above rated wind speed (12 m/s), and above rated wind speed (14 m/s). The linear models are, in fact, identified as the Bladed model generates input and state perturbations, and records the resulting variations in the state derivatives and selected outputs to finally derive a linearised model of the turbine in state-space form [13]. In state space form, they have the following form:

$$\Delta\dot{\mathbf{x}}(t) = A\Delta\mathbf{x}(t) + B\Delta\mathbf{u}_T(t)$$
$$\Delta\mathbf{y}(t) = C\Delta\mathbf{x}(t) + D\Delta\mathbf{u}_T(t) \tag{13}$$

where A, B, C, and D denote the state space matrices. $\Delta\mathbf{y}(t) \in \mathbb{R}^n$, $\Delta\mathbf{u}_T(t) \in \mathbb{R}^m$ and $\Delta\mathbf{x}(t) \in \mathbb{R}^r$ (where n and m are respectively 10 and 3 at each mean wind speed, and r is 30 at 10 m/s and 26 at 12 m/s and 14 m/s) are defined as

$$\Delta\mathbf{y}(t) = \mathbf{y}(t) - \mathbf{y}_{op}(t) \tag{14}$$
$$\Delta\mathbf{u}_T(t) = \mathbf{u}_T(t) - \mathbf{u}_{T,op}(t) \tag{15}$$
$$\Delta\mathbf{x}(t) = \mathbf{x}(t) - \mathbf{x}_{op}(t) \tag{16}$$

$\mathbf{y}(t)$, $\mathbf{u}_T(t)$, and $\mathbf{x}(t)$ represent the output, input, and states, respectively, and $\mathbf{y}_{op}(t)$, $\mathbf{u}_{T,op}(t)$, and $\mathbf{x}_{op}(t)$ are the operating points around which the models are linearised. The resulting Matlab/SIMULINK simulation model is depicted in Fig. 2.

There are 10 outputs for the linear models: measured generator speed, nacelle x-acceleration (also known as tower acceleration), nacelle y-acceleration, generator torque, pitch angle, blade pitch rate, nominal pitch angle, electrical power, generator speed, rotor speed, blade flapwise bending moment, and blade edgewise bending moment. The 3 inputs are wind speed, pitch angle, and generator torque demand.

When designing a generator torque controller for the below rated model, wind speed among the inputs, $\mathbf{u}_T(t)$, is considered to be a disturbance, $\mathbf{d}(t) \in \mathbb{R}^1$, and pitch angle set to zero modifying (13) as follows.

$$\Delta\dot{\mathbf{x}}(t) = A\Delta\mathbf{x}(t) + B_u\Delta u(t) + B_d\Delta\mathbf{d}(t)$$
$$\Delta\mathbf{y}(t) = C\Delta\mathbf{x}(t) + D_u\Delta u(t) + D_d\Delta\mathbf{d}(t) \tag{17}$$

where the input, $u(t) \in \mathbb{R}^1$, is now generator torque (or generator torque demand) only.

When designing pitch controllers for the just above and above rated models, $u(t)$ would be pitch angle only, wind speed is treated as a disturbance, and generator torque is set to a constant value. This is also manifested in Fig. 2. Therefore, MPC controllers utilise the following SISO equations:

$$\Delta\dot{\mathbf{x}}(t) = A\Delta\mathbf{x}(t) + B_u\Delta u(t)$$
$$\Delta y_g(t) = C_g\Delta\mathbf{x}(t) + D_{u,g}\Delta u(t) \tag{18}$$

where $y_g(t) \in \mathbb{R}^1$ denotes generator speed, and $D_{u,g}$ zero.

To wit, the torque (at 10 m/s) and pitch (at 12 and 14 m/s) controllers control generator speed by varying generator torque demand and by active pitching, respectively.

As previously mentioned, these models are referred to as Models A throughout the paper. The open-loop frequency responses of these models for mean wind speeds of 10, 12, and 14 m/s are depicted in Figs. 3 and 4, in comparison to the open-loop frequency responses of the models introduced in the following section (i.e. Models B).

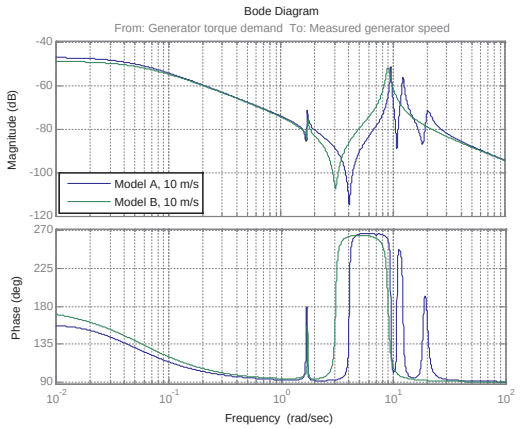

Fig. 3. Frequency responses of Model A and Model B at a mean wind speed of 10 m/s.

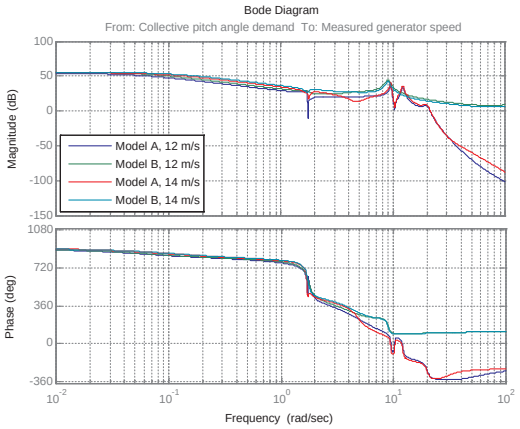

Fig. 4. Frequency responses of Models A and Models B at mean wind speeds of 12 and 14 m/s.

C. Wind Turbine Linear Models B (linearisation via symbolic differentiation)

The nonlinear model equations provided in [7] are linearised via symbolic differentiation (Taylor series expansion) in this section. The parameters of the same turbine as the one used to derive Models A (i.e. Supergen 5MW exemplar turbine) are exploited. Being only 12$^{\text{th}}$ order for at 10 m/s and 11$^{\text{th}}$ order at 12 and 14 m/s, they are much simpler models than Models A. As depicted in Fig. 2, in below rated wind speed (i.e., at 10 m/s) the control input (i.e. input to the turbine from the controller) is torque demand, while in above rated wind speed (i.e., at 12 and 14 m/s) the control input is pitch demand. Hence, it is a plausible outcome that the orders of the models are different. These models are also in state space form, and referred to as Models B throughout the paper, as previously mentioned. The open-loop frequency responses for 10, 12, and 14 m/s are depicted in Figs. 3 and 4, in comparison to the open-loop frequency responses of Models A from Section II-B.

The inputs are same as Models A, but there are 2 outputs only: measured generator speed and nacelle x-acceleration.

III. Model Predictive Control

MPC is briefly revised in this section and designed based on both Models A and Models B to investigate the controllers' dependence on the choice of linear models used during the design process. The Models A-based controllers are applied to Models B, and the Models B-based controllers to Models A. The differences between these models provide a degree of model-plant mismatch to test the robustness of design.

For the following state-space model, which can be obtained by discretising the continuous model in (18),

$$\mathbf{x}_{k+1} = A\mathbf{x}_k + B_u u_k \tag{19}$$

$$y_{k+1} = C_g \mathbf{x}_{k+1} \tag{20}$$

the prediction equations for MPC can be derived as [14] (note that the D state-space matrix is zero since no direct feedthrough is allowed in MPC)

$$\underset{\rightarrow}{\mathbf{x}} = P_{xx}\mathbf{x}_k + H_{xx}\underset{\rightarrow}{u} \tag{21}$$

$$\underset{\rightarrow}{y} = H\mathbf{x}_{k+1} \tag{22}$$

where H_{xx}, H and P_{xx} are the prediction matrices [14] and $\underset{\rightarrow}{u}$ is a column vector as follows:

$$\left[u_{k+1}, u_{k+2}, \ldots, u_{k+n_{u-1}}, u_{k+n_u}, u_{k+n_u}, \ldots, u_{k+n_u}\right]^T \tag{23}$$

MPC requires the prediction horizon, n_y, not to be smaller than the control horizon, n_u; that is, $n_u \leq n_y$.

The control solution can be attained with minimising the following objective function:

$$J = \left\| r - \mathbf{H}\underset{\rightarrow}{u} - \mathbf{P}\hat{x}_k - \mathbf{L}d \right\|_2^2 + \lambda \left\| \underset{\rightarrow}{u} \right\|_2^2 \tag{24}$$

subject to the following constraints

$$\underline{u}_i \leq u_i \leq \overline{u}_i \tag{25}$$

$$\Delta\underline{u}_i \leq \Delta u_i \leq \Delta\overline{u}_i \tag{26}$$

where $\overline{u}_i$ denotes the upper limit on u_i, $\underline{u}_i$ the lower limit, r the reference signal, $\mathbf{L}$ a vector of ones, whose size is simply dependent on the prediction horizon, and Δu_i the rate of change of input. The offset $d = y - \hat{y}$ is included to give unbiased predictions and offset correction. The first $\|.\|_2^2$ term is to reduce the reference tracking error and the second $\|.\|_2^2$ term to reduce the control action. Therefore, λ provides a trade-off between these two conflicting problems. $\hat{x}_k$ comes from the internal model here, but a state estimator such as the Kalman filter could also be utilised. For the optimisation, the Matlab function, "quadprog" (the interior-point-convex algorithm) is employed.

The MPC controllers designed based on Models A and Models B at 10, 12 and 14 m/s are respectively applied to Models B and Models A in Matlab/SIMULINK as previously described. The measured outputs (i.e. generator speed) are

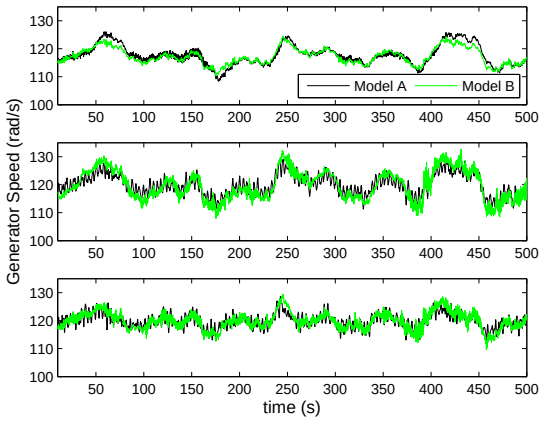

Fig. 5. MPC based on Models A and Models B; generator speed (output); time responses for mean wind speeds of 10 m/s, 12 m/s, and 14 m/s.

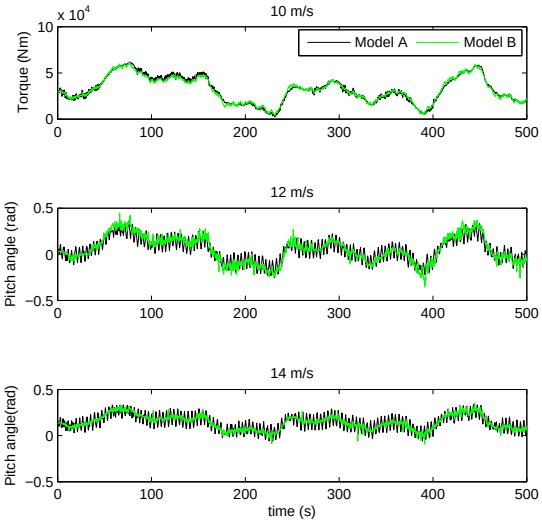

Fig. 6. MPC based on Models A and Models B; torque demand (10 m/s) and pitch (12 and 14 m/s) (control input); time responses for mean wind speeds of 10 m/s, 12 m/s, and 14 m/s.

depicted in Fig. 5. The time responses for the Models B-based controllers at each mean wind speed are satisfactory as the fluctuations remain well below 12 %, which is often within the controller design specification. Although the fluctuations remain well below 12 % for the Models A-based controllers also, sustained oscillation (at frequency of around 5.5 rad/s) can be observed at mean wind speeds of 12 and 14 m/s. It would result in increased loads on the rotor that would propagate down the power-train and impact on the drive train components, e.g. gearbox and shaft. The cause of this is explained with the frequency response in Fig. 8 below.

Torque demand and pitch angle (control inputs) are also presented in Fig. 6. As mentioned previously, the turbine operates in mode 3 at 10 m/s and in mode 4 at 12 and 14 m/s. Generator speed is controlled by varying torque in mode 3 and by active pitching in mode 4. As such, fluctuation on the control inputs is not as restricted as generator speed, the output. Pitch angle ranges from -0.0873 to 0.6109 rad (-5° to 35°) for the turbine considered in this paper.

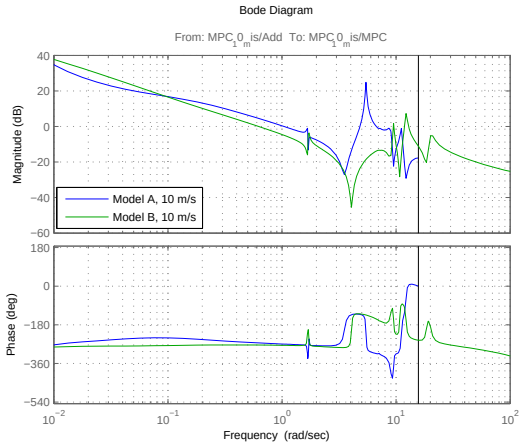

Fig. 7. MPC based on Models A and Models B for a mean wind speed of 10 m/s; open loop frequency responses; T_s=0.2 s (sampling time) for Models A and T_s=0.02 s for Models B.

The open-loop frequency responses for the Models A-based controllers demonstrate poorer results in comparison to the Models B-based controllers as depicted in Figs. 7 and 8. The open-loop system of a controller in this paper is referred to as the product of the process (i.e. the turbine model) and the controller open-loop. With information obtained from the open-loop responses, such as gain crossover frequency, phase margin, etc, the response of the close-loop system, including the size of the control action, sensitivity to uncertainty, and stability, can be speculated.

The Models A-based controllers are more sensitive to sampling time, T_s, and 0.2 s needs to be chosen to improve the results. The vertical lines that appear at 20 rad/s in the figures are due to discretisation with this sampling time. However, the Models B-based controllers are less sensitive to sampling time, and a smaller sampling time, i.e. 0.02 s, could successfully be exploited.

At a mean wind speed of 10 m/s, Fig. 7 depicts that the gain crossover frequencies of the Model A and B-based controllers are approximately 1 and 0.6 rad/s, respectively. Note that Control System Toolbox™ in Matlab is exploited here for producing open-loop frequency responses in bode plots. Due to the characteristics of wind, the controllers should be tuned to give a gain crossover frequency in the range of 0.6 to 2 rad/s [15]. Gain crossover frequencies over this range may lead to large control action, hence actuator saturation, especially in high wind speeds. Gain crossover frequencies below this range could lead to too slow control action. Both controllers are satisfactory in terms of the gain crossover frequency.

However, the peaks produced by the Models A-based controller cross over 0 dB, indicating that the controller would

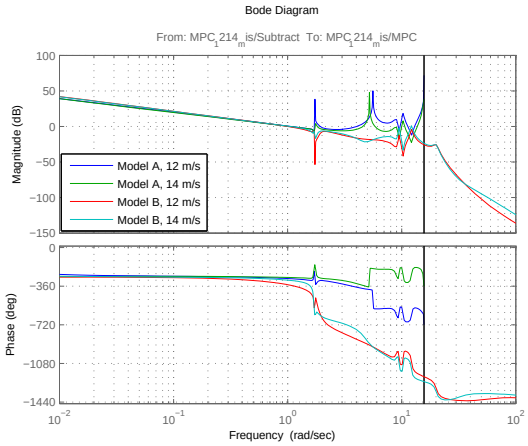

Fig. 8. MPC based on Models A and Models B at mean wind speeds of 12 and 14 m/s; open loop frequency responses; T_s=0.2 s (sampling time) for Models A and T_s=0.02 s for Models B.

be sensitive to uncertainty and noise. When the Models B-based controller is employed, the magnitudes of the peaks are reduced. The controllers should be tuned to ensure that the peaks at high frequencies are kept as small as possible. Moreover, phase margins for both controllers are some 90°, indicating that their closed-loop responses would be stable – note that the MPC controllers incorporate a positive feedback.

For mean wind speeds of 12 and 14 m/s, Fig. 8 depicts that the gain crossover frequencies are approximately 1 rad/s for both controllers. However, the peaks from the Models A-based controllers remain mostly above 0 dB, indicating that the controllers would be sensitive to uncertainty and noise. The peaks at around 5.5 rad/s in particular cause the sustained oscillation that is observed in the time response in Fig. 5. The responses of the Models B-based controllers demonstrate significantly improved results keeping most of the peaks below 0 dB, hence no sustained oscillation at the specific frequencies is visible in the time response. Phase margins are around 72° (12 m/s) and 82° (14 m/s) for the Models A-based controllers and 11° (12 m/s) and 57° (14 m/s) for the Models B-based controllers, indicating that their closed-loop responses would be stable.

IV. Conclusion

Two linear dynamic models (including wind speed models) of the Supergen 5MW exemplar turbine are constructed for three operating points, below rated wind speed (10 m/s), just above rated wind speed (12 m/s) and above rated wind speed (14 m/s). One is obtained in Bladed using its linearisation toolbox, and the other using the standard linearisation method via the Taylor series expansion. In order to investigate the MPCs' dependence on the choice of linear model used during the design process, the controllers are designed for the three wind speeds using the latter and the performance achieved by the controllers assessed using the former, and vice versa. The differences between these models provide a degree of model-plant mismatch to test the robustness of design.

The properties of the MPC controllers are highly dependent on the choice of linear model used during the design process. The simulation results demonstrate improved control performance when the MPC controllers are tuned based on Models B (the models linearised via the Taylor series expansion), which are simpler models; recall that Models A are 30$^{\text{th}}$ order at 10 m/s and 26$^{\text{th}}$ order at 12 and 14 m/s, while Models B are 12$^{\text{th}}$ order at 10 m/s and 11$^{\text{th}}$ order at 12 and 14 m/s. Models A, being high-order, have a tendency to cause the controllers to become over-aggressive, i.e. active at higher frequencies, and to lack robustness. It is therefore recommended that the control design models be kept as simple as possible when designing MPC controllers for wind turbines.

Acknowledgment

The authors wish to acknowledge the support of the EPSRC for the Supergen Wind Energy Technologies Consortium, grant number EP/H018662/1.

References

[1] N. Luo, Y. Vidal, and L. Acho, *Wind Turbine Control and Monitoring*. Springer, 2014.
[2] A. Chatzopoulos, "Full Envelope Wind Turbine Controller Design for Power Regulation and Tower Load Reduction," Ph.D. dissertation, University of Strathclyde, 2011.
[3] A. I. Grancharova and T. A. Johansen, *Explicit Nonlinear Model Predictive Control: Theory and Applications*. Springer, 2012.
[4] H. trentelman, A. A. Stoorvogel, and M. Hautus, *Control Theory for Linear Systems (Communications and Control Engineering)*. Springer, 2012.
[5] S. Skogestad and I. Postlethwaite, *Multivariable Feedback Control: Analysis and Design*, 2nd ed. Wiley, 2005.
[6] C. Brosilow and B. Joseph, *Techniques of Model-based Control*. Prentice Hall Professional, 2002.
[7] W. Leithead and B. Connor, "Control of variable speed wind turbines: Dynamic models," *International Journal of Control*, vol. 73: 13, pp. 1173 – 1188, 2000.
[8] S. Hur and W. E. Leithead, "Control of a Wind Turbine," Industrial Control Centre, Department of Electronic and Electrical Engineering, University of Strathclyde, Tech. Rep., 2014.
[9] W. E. Leithead and B. Connor, "Control of variable speed wind turbines: design task," *International Journal of Control*, vol. 13, pp. 1189–1212, 2000.
[10] W. E. Leithead, "Effective wind speed models for simple wind turbine simulations," in *Proceedings of* 14^{th} *British Wind Energy Association (BWEA) Conference, Nottingham*, 1992.
[11] V. W. Neilson, "Individual Blade Control for Fatigue Load Reduction of Large-scaled Wind Turbines: Theory and Modelling," Master's thesis, Department of Electronic and Electrical Engineering, University of Strathclyde, 2010.
[12] I. Munteanu, A. I. Bratcu, N.-A. Cutululis, and E. Ceangă, *Optimal Control of Wind Energy Systems: Towards a Global Approach*. Springer, 2007.
[13] *Bladed User Manual v4.3*.
[14] J. A. Rossiter, *Model-Based Predictive Control: a Practical Approach*. CRC Press, 2005.
[15] D. J. Leith and W. E. Leithead, "Appropriate realization of gain-scheduled controllers with application to wind turbine regulation," *International Journal of Control*, vol. 65(2), 1996.